

pubs.acs.org/cm Article

Cleanly Removable Surfactant for Carbon Nanotubes

Chiyu Zhang, Peng Wang, Benjamin Barnes, Jacob Fortner, and YuHuang Wang*



Cite This: Chem. Mater. 2021, 33, 4551-4557



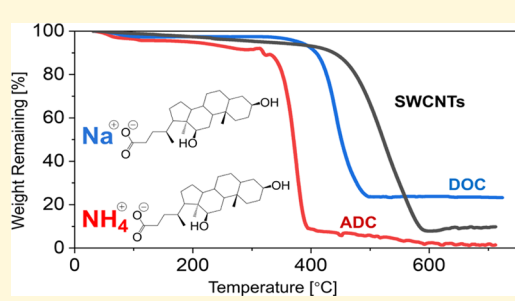
ACCESS

Metrics & More

Article Recommendations

Supporting Information

ABSTRACT: Surfactants, molecular surface-active agents, are widely used to stabilize single-walled carbon nanotubes (SWCNTs) and many other nanomaterials in water to facilitate solution processing and device integration. However, it is notoriously difficult to cleanly remove surfactants when they are no longer needed. Even high-temperature thermal annealing leaves residues that can degrade the otherwise remarkable electrical and optical properties of SWCNTs. Moreover, thermal annealing damages smaller-diameter nanotubes (<1 nm) due to aggressive oxidation at elevated temperatures. To address this challenge, we report the synthesis of ammonium deoxycholate (ADC) that can be cleanly removed at a relatively low temperature that preserves the SWCNT structure. We find that ADC is as efficient as sodium deoxycholate (a commonly used



surfactant featuring the same anion) at individually dispersing SWCNTs in water. However, replacing the metal cation (Na⁺) of sodium deoxycholate with ammonium (NH₄⁺) to form ADC reduces the peak thermal decomposition temperature by nearly 70 °C. Furthermore, unlike sodium deoxycholate, thermal annealing of ADC in Ar leaves behind only a small amount of carbonized residue that can be cleanly decomposed in the presence of 5% O_2 at 400 °C, a condition that preserves SWCNTs even with a small diameter of just 0.76 nm. This work uncovers the chemical origin of residues from the thermal annealing of surfactant-processed carbon nanomaterials and provides an unexpectedly simple solution to this persistent challenge.

■ INTRODUCTION

Single-walled carbon nanotubes (SWCNTs) are a family of cylindrical carbon allotropes that exhibit extraordinary electrical, optical, and mechanical properties. 1-3 Because these carbon nanomaterials are synthesized as a heterogeneous mixture of different structures that bundle strongly, polymers $^{4-8}$ and surfactants, $^{9-11}$ such as sodium dodecyl sulfate (SDS) and sodium deoxycholate (DOC), are widely used to disperse SWCNTs in solution for subsequent purification, 12 fiber spinning, 13 ink formulation, 14 and the fabrication of highperformance nanoelectronic devices. 10 However, after solution processing, surfactants become unwanted contaminants. For example, surfactants that remain on the surfaces of SWCNTs can scatter electrons and interfere with electrical transport in thin-film devices, significantly reducing the signal-to-noise ratio, conductivity, and sensitivity. Similarly, residual surfactant molecules can degrade the optical performance of SWCNTs, resulting in lower fluorescence quantum yields and broadened absorption peaks. ^{18–21} Surfactant adsorption also interferes with the interaction of SWCNTs with other molecules, including obstructing active sites on the surface of sensors²² and preventing reactant access for nanotube functionalization.²³ Therefore, while surfactants are often necessary to utilize SWCNTs, improved surfactant-removing methods are needed to ensure optimal performance.

Multiple approaches have been investigated for the removal of polymers and surfactants from SWCNTs, including rinsing with organic solvents, ^{24–26} acidic oxidation, ^{26–28} and annealing

in inert^{28–30} or oxygen atmospheres.^{31,32} For example, acetone and acetonitrile have been shown to interrupt the SWCNTsurfactant interaction, thereby releasing surfactants from nanotube surfaces. However, this technique also causes large nanotube bundles that negatively impact the SWCNT functionality as well as weaken the material's intrinsic photoluminescence (PL) efficiency. 24,33 Moreover, it has been found that surfactant layers tightly clinging to SWCNT sidewalls cannot be completely removed by simply rinsing. 24,26,34 Although harsher methods, such as acidic treatment (e.g., nitric acid), can efficiently etch obstinate residues, 26,27 the strong oxidative nature of such treatments can also induce covalent defects in nanotube sidewalls.²⁸ Alternatively, annealing has been routinely used to increase the conductivity of devices fabricated from SWCNTs that are solution-processed using surfactants and polymers. However, residues often remain after annealing, which limit the efficacy of this approach. 22,31,36-39

In this work, we address this need for "clean" solution-processed SWCNTs by designing and synthesizing a new SWCNT surfactant—ammonium deoxycholate (ADC)—that

Received: March 18, 2021 Revised: May 26, 2021 Published: June 10, 2021





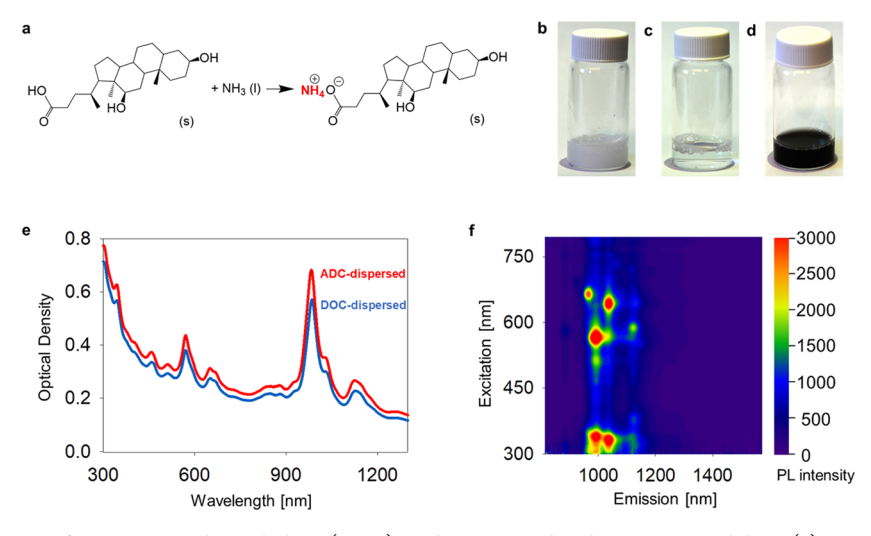


Figure 1. One-pot synthesis of ammonium deoxycholate (ADC) and its nanotube dispersion capability. (a) One-pot reaction scheme for synthesizing ADC by mixing deoxycholic acid and liquid ammonia. Photographs of the (b) 1 wt% deoxycholic acid suspension, (c) 1 wt% ADC solution, and (d) aqueous solution of SG65 SWCNTs stabilized by 1 wt % ADC. (e) Ultraviolet—visible—near infrared (UV—vis—NIR) absorption spectrum of individual SWCNTs dispersed in 1 wt % ADC (red) and DOC (blue) aqueous solutions. (f) Excitation-emission PL map of SWCNTs dispersed in 1 wt % ADC aqueous solution, showing PL signatures characteristic of individually dispersed SWCNTs.

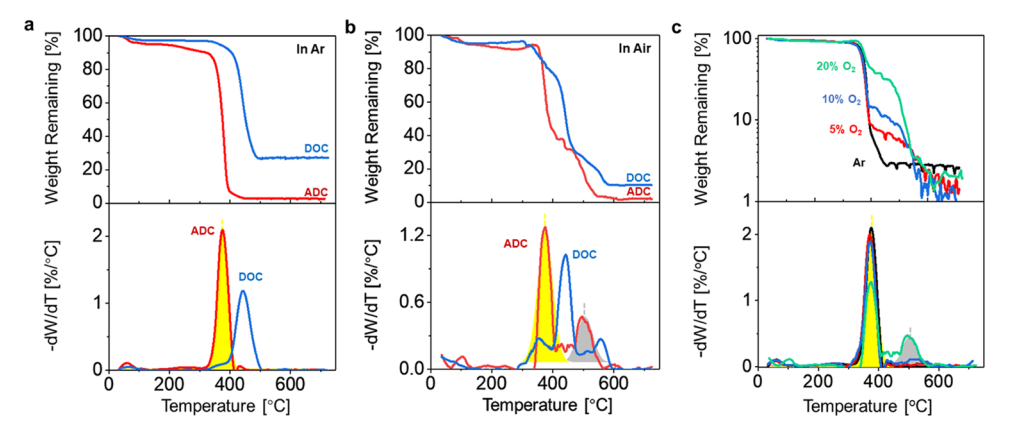


Figure 2. Heating removes ADC at low temperature. TGA and derivative TGA (dTGA) plots of ADC (red) and DOC (blue) in (a) Ar and (b) air, in which the final residual mass of ADC was nearly zero (\sim 2%) and the $T_{\rm max}$ of ADC was significantly lower than DOCs in both atmospheres. (c) TGA and dTGA plots of ADC in Ar (black), 5% O₂ (red), 10% O₂ (blue), and 20% O₂ (air, green). The yellow-shaded peaks in the dTGA curves indicate that the $T_{\rm max}$ of ADC in both Ar and air is 375 °C. The gray-shaded peaks may correspond to thermally stable intermediates that are produced from annealing ADC in the presence of oxygen.

can be thermally removed at significantly lower temperatures. We find that this surfactant can disperse SWCNTs up to 10 mg/mL (in 1 wt % ADC aqueous solution), comparable to DOC, 11 which is known for its high dispersion efficiency and features the same amphiphilic anion. More importantly, ADC can be thermally removed, with the ammonium (NH₄⁺) cation decomposing to gaseous ammonia under heating. Thermogravimetric (TGA) analysis reveals that the ADC surfactant can be thermally decomposed at a significantly lower temperature, by 70 °C, than DOC. By first annealing in Ar at low temperature (400 °C) and then removing the small amount of remaining residue with 5% O2 at the same heating condition, $98.5 \pm 0.6\%$ of the ADC can be removed from SWCNTs. In contrast, only 77.0 \pm 0.4% of DOC (containing Na⁺) can be removed under these conditions, with an obstinate black char remaining. Transmission electron microscopy (TEM) directly confirms the cleanness of the processed SWCNTs. Furthermore, the SWCNT crystalline structure remains intact, ensuring that the material's intrinsic properties are retained.

■ RESULTS AND DISCUSSION

We synthesized ADC by reacting deoxycholic acid with an excess amount of liquid ammonia, yielding ADC as a solid white powder (Figure 1a). The solubility of deoxycholic acid in water is merely ~43.6 mg/L (Figure 1b), 40 while the synthesized solid ADC shows an excellent solubility of \sim 21 000 mg/L at pH = 7 (Figure 1c). The successful synthesis of ADC is supported by both direct analysis in real-time (DART) mass spectrometry and Fourier transform infrared (FTIR) spectroscopy. DART mass spectrum of the synthesized ADC displays a peak at m/z 410.3, corresponding to the protonated ADC molecule (Figure S6a). In FTIR, the synthesized ADC features a strong N-H bending peak at 1543 cm⁻¹ and the N-H stretching at 3390 cm⁻¹, which are spectral signatures of ammonium moieties, while the broad O-H stretching peak of -COOH group of the deoxycholic acid precursor at 3334 cm⁻¹ disappears (Figure S1).

To investigate ADC's dispersion ability for SWCNTs, we first mixed CoMoCAT SG65 SWCNTs with 1 wt % ADC

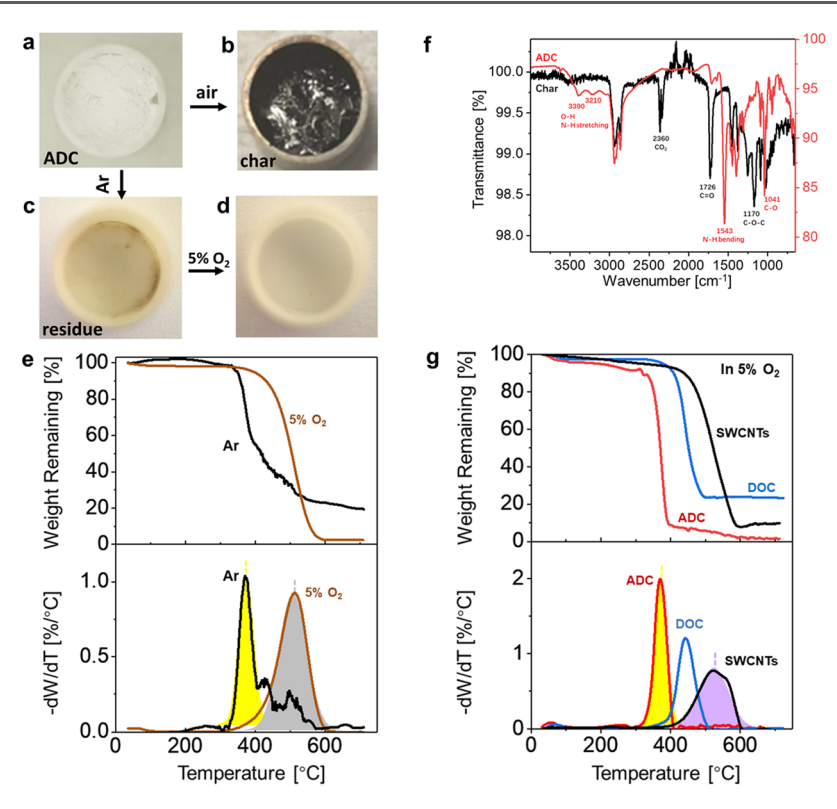


Figure 3. Origin of the surfactant residue after annealing. Photographs of the (a) initial 30 mg of ADC solid and (b) the char obtained after annealing the ADC in air at 400 °C for 1 h. (c) Residue after annealing ADC in Ar at 400 °C for 1 h, (d) which can be removed by subsequent annealing at 5% O_2 at 400 °C for 1 h. (e) TGA and dTGA plots of the char annealed in either Ar (black) or 5% O_2 (brown). The yellow-shaded peak in the dTGA plot corresponds to the removal of ADC, while the gray-shaded peak indicates that the $T_{\rm max}$ of the char in O_2 is 509 °C. (f) FTIR spectra of the ADC (red) and char (black), showing that ADC is oxidized below 400 °C, forming C=O and C-O-C bonds. (g) TGA and dTGA plots of SG65 SWCNTs (black), ADC (red), and DOC (blue) in 5% O_2 showing that the $T_{\rm max}$ of ADC (yellow shaded, 375 °C) and $T_{\rm max}$ of SG65 SWCNTs (purple shaded, 523 °C) are separated. Therefore, the removal of ADC at 400 °C should not damage SG65 SWCNTs. In contrast, the combustion peaks of DOC and SG65 SWCNTs significantly overlap, suggesting that the DOC cannot be fully removed without also oxidizing nanotubes.

aqueous solution followed by tip sonication and ultracentrifugation (see the Experimental Section for details). Nanotubes readily dispersed to form a stable, homogenous SWCNT suspension (Figure 1d). We then used ultravioletvisible—near infrared (UV-vis-NIR) absorption spectroscopy (Figure 1e) and PL excitation-emission mapping (Figure 1f) to characterize the dispersion quality of the ADC-wrapped SWCNTs. The sharp absorption peaks originating from the SWCNT van Hove singularities and strong PL intensity of the dispersion indicated the SWCNTs were well-individualized in the aqueous solution rather than bundled.9 The SWCNT suspension was stable for more than 1 year (Figure S2a,b). We note that ADC can disperse SWCNTs at a concentration of at least 10 mg/mL (Figure S3), which is similar to that of DOC, 11 one of the most efficient and commonly used surfactants for SWCNT dispersion. We note that excess ammonium hydroxide can be introduced into the ADC aqueous solution without affecting its dispersion ability and the properties of dispersed SWCNTs (Figure S2c,d), since ammonia is a weak base.

We then compared the thermal stability of the solid ADC with DOC by heating the materials in Ar (99.999%) and air (20% $O_2)$ atmospheres using TGA (Figure 2a,b). A higher content of ADC was removed at a lower temperature than DOC in both atmospheres, with a maximum decomposition rate at $\sim\!375\,^{\circ}\mathrm{C}$ (T $_{\mathrm{max}}$ yellow-shaded peaks), leaving nearly zero residual mass at 700 °C (2.1 \pm 1.7% in Ar and 1.6 \pm 2.0%

in air). In contrast, the $T_{\rm max}$ of DOC was as high as ~445 °C in the two atmospheres. More significantly, 93.6 \pm 0.3 and 60.7 \pm 3.5% of ADC was removed in Ar and air, respectively, at temperatures lower than 400 °C, while only 9.1 \pm 0.6 and 24.0 \pm 1.0% of DOC was decomposed at the same annealing conditions. These results suggest that the thermal stability of deoxycholate salt derivatives can be tailored by replacing the metal cation (Na⁺) with ammonium (NH₄⁺). The difference in the decomposition temperature of ADC and DOC can be attributed to the fact that ADC can decompose into deoxycholic acid and a gaseous ammonia leaving group, while sodium ions cannot leave in the gas phase as Na due to its highly reactive nature, as contrasted by the equations below.

$$C_{23}H_{39}O_2COO^-NH_4^+ \rightarrow C_{23}H_{39}O_2COOH + NH_3\uparrow$$
 (1)

$$C_{23}H_{39}O_2COO^-Na^+ \leftrightarrow C_{23}H_{39}O_2COO + Na$$

The lower decomposition temperature of ADC may also allow us to selectively remove the surfactant while minimizing damage to the SWCNT structure.

Additionally, we note that a second peak appears in the derivative TGA (dTGA) curve of the air-annealed ADC thermogram at ~ 509 °C (Figure 2a, gray-shaded peak), suggesting the production of thermally stable intermediates when O_2 is involved in the annealing process. To investigate how O_2 affects the removal of ADC, we annealed the surfactant in atmospheres of different O_2 concentrations (0–20%). With

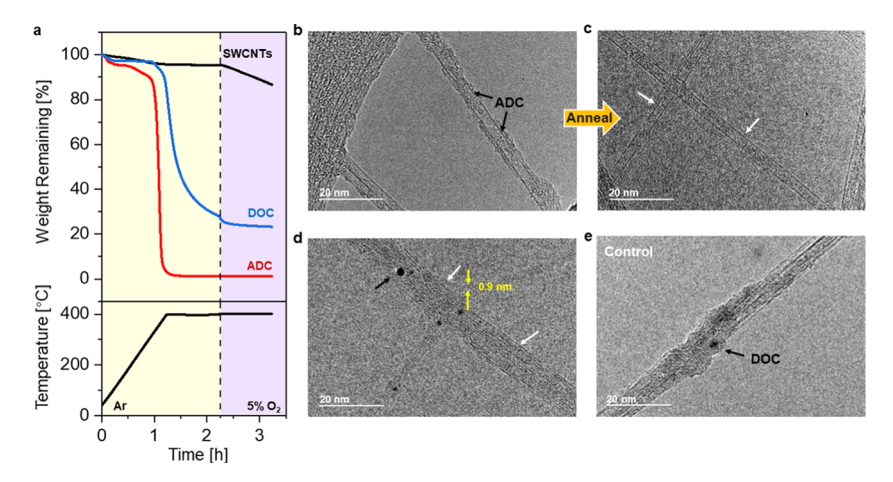


Figure 4. Cleanness of ADC-dispersed SWCNTs after the two-step annealing process. (a) TGA plots of SG65 SWCNTs (black), DOC (blue), and ADC (red) at 400 °C in Ar (yellow region) and then 5% O_2 (purple region) at 400 °C. The temperature profile is shown below. (b, c) TEM images of EC2.0 SWCNTs (\sim 2 to 3 nm) dispersed by 1 wt % ADC (b) before and (c) after the two-step annealing process. (d) Annealed SG65 SWCNTs (\sim 0.78 nm) dispersed by 1 wt % ADC, demonstrating the clean nanotube surfaces and intact SWCNT structures. (e) Annealed EC2.0 SWCNTs dispersed by 1 wt % DOC solution as a control, showing unremoved DOC residue clinging to the surface of the SWCNTs. The black arrows show surfactants and their residues. The white arrows indicate clean straight SWCNT walls after annealing.

increasing oxygen, the intensity of the TGA shoulder between 390 and 550 °C increases (Figure 2c), which indicates that ADC is reacting with $\rm O_2$ and generating more intermediate products. These intermediates are then decomposed at higher temperatures ($T_{\rm max} > 500$ °C).

To better understand this annealing process, we visually observed these intermediates by heating the white ADC powder (Figure 3a) to 400 °C for 1 h in 20% O₂ (air), which produced a large amount of brownish char (that appeared black in large quantities; Figure 3b). In contrast, only a small amount of brownish residue remained after annealing the ADC in Ar under the same condition (Figure 3c). Notably, this fairly clean removal of ADC in Ar is quite different from its sodium variant (DOC), which produced a significant amount of black char under the same annealing conditions (Figure S4). This difference can be explained based on that while heating ADC in Ar a white solid condenses on the furnace wall of the cooling region downstream of the heater (Figure S5). Characterization using DART mass spectrometry reveals that this solid features a peak at m/z 392.4, which corresponds to the mass of ADC minus one ammonia molecule (Figure S6). These results suggest the ionic structure of ADC thermally decomposes under heat treatment, with the ammonium ion leaving in the form of gaseous ammonia, while the carbon skeleton of the deoxycholic anion remains intact. However, ADC cannot be completely removed through sublimation, as a small amount of brownish residue remains after Ar annealing (Figure 3c). This residue is the same brownish color as that of the char produced from the air-annealed ADC sample (Figure 3b). The similarity between these materials suggests that the residue after Ar annealing may be the same compound as the char, generated by O₂ impurities in the Ar gas flow.

To investigate how to remove this residue, we used TGA to characterize the char produced from the air-annealed ADC (Figure 3e). After heating in Ar, 20% of the char remained even at 700 °C, indicating that it cannot completely decompose into gaseous species under these conditions. The loss of mass that was observed is potentially due to the removal of unreacted ADC trapped in the char as the TGA curve shows the typical $T_{\rm max}$ of ADC in Ar (yellow-shaded peak, ~375 °C).

The chemical origin of the high thermal stability of the char is hinted by its FTIR spectrum, which shows strong C=O (1726 cm⁻¹) and C-O-C (1170 cm⁻¹) stretching peaks that are absent in the ADC spectrum (Figure 3f). These results suggest a large amount of C=O (possibly from the oxidation of -OH groups on the six-carbon rings of deoxycholate anions) and C-O-C bonds (possibly from the loss of one water molecule between -OH groups on separate ADC molecules, which could cross-link the ADC molecules) are formed when ADC reacts with air below 400 °C, resulting in a high thermal stability that prevents the char from being removed by Ar annealing alone. However, when we anneal the char in 5% O₂ (Figure 3e), only 2.4% mass remains, indicating that the char can be etched by O₂ though it requires a high temperature of 509 °C ($T_{\rm max}$ gray-shaded peak).

While the ADC char can be removed by heating in oxygen, it is important to investigate whether SWCNTs could survive in similar conditions without degradation. SWCNTs feature a broad range of diameters and chiralities, and nanotubes with smaller diameters are generally more susceptible to degradation at high temperatures due to strain-induced reactivity.⁴¹ SG65 SWCNTs (synthesized by the CoMoCAT process) mainly consist of small-diameter nanotubes (\sim 0.78 nm), which are less thermally stable than the larger diameter nanotubes found in EC1.5 (\sim 1 to 3 nm) and EC2.0 (\sim 2 to 3 nm) SWCNT sources (Figure S7), and therefore represent the lower limit for the heat treatment condition. We conducted TGA on SG65 SWCNTs in 5% O2 and compared the degradation temperature to that of DOC and ADC (Figure 3g). The wide dTGA peak of the SWCNTs indicates that nanotubes begin to thermally decompose at 400 $^{\circ}\text{C}\text{,}$ with the highest decomposition rate occurring at 523 °C. The significant overlap of the decomposition temperature between SWCNTs and DOC (T_{max} = 445 °C) makes selective removal of the surfactant by thermal annealing impossible without also damaging SWCNTs. In contrast, the narrow dTGA peak of ADC $(T_{\text{max}} = 375 \text{ °C})$ under the same conditions is well separated from the SWCNT decomposition peak, which allows us to remove the small amount of ADC char by heating in oxygen at 400 °C.

These findings suggest a two-step process to successfully remove ADC. First, we must avoid the formation of a large amount of char by annealing in Ar. We find that after annealing ADC in Ar at 400 °C for 1 h, the majority of ADC (98.1%) is sublimated and the small amount of residue that remains as char, which is induced possibly due to oxygen impurities in the Ar gas flow, can subsequently be removed by heating the material in 5% $\rm O_2$ at a relatively low temperature of 400 °C for 1 h (Figure 3d), under which conditions the nanotube structure is preserved.

TGA confirms that ADC can be cleanly removed from SWCNTs using this two-step annealing process, in which 98.5 \pm 0.6% of ADC is eliminated, while only 77.0 \pm 0.4% of DOC is removed under the same conditions (Figure 4a). These findings are further supported by TEM. Figure 4b shows ADCdispersed EC2.0 SWCNTs (the large diameter of which helps in observing the nanotube morphology). After the two-step annealing treatment, ADC is completely removed and SWCNTs feature clean and smooth walls, as shown in Figure 4c. The annealing method is also applicable to other species of SWCNTs (Figure S8). In particular, even small-diameter SWCNTs (0.9 nm) survive and exhibit a clean surface (Figure 4d). The cleanliness of the annealed SWCNTs is comparable to those dispersed in chloroform by tip sonication without the use of any surfactant (Figure S9). In contrast, DOC leaves behind a large amount of residue clustered on sidewalls after annealing (Figure 4e). Raman spectroscopy further confirms that the ADC surfactant is selectively removed with minimal damage to even small-diameter nanotubes (Figure S10), as evidenced by the low D/G ratio. We note that the electrical conductance of metallic nanotubes (EC1.5) increases by up to 100-folds after the annealing (Figure S11). The PL of nanotubes remains observable from a thin film of mixed small-diameter SG65 nanotubes but becomes dimmed by ~10fold (Figure S12), which can be attributed to the removal of surfactant molecules that separate semiconducting nanotubes from the metallic ones. These findings unambiguously reveal that ADC can be cleanly and selectively removed from SWCNTs of various diameters without damaging the graphitic structure.

CONCLUSIONS

In conclusion, we report the synthesis of ADC, a new SWCNT surfactant that can be cleanly removed by thermal annealing without damaging even small-diameter SWCNTs. ADC disperses SWCNTs as efficiently as DOC, which features the same anion. However, by replacing the Na⁺ cation with NH₄⁺, we find ADC thermally decomposes at a significantly lower temperature (by 70 °C) and can be almost completely removed through a sublimation mechanism in Ar without the formation of an obstinate char. We further find that the formation of char occurs due to incomplete oxidation of the surfactant, which explains the chemical origin of similar residue leftover from the thermal annealing of surfactant-processed carbon nanotubes. To completely avoid O2-induced char, we developed a two-step protocol that involves first annealing in Ar at 400 °C to vaporize the majority of the surfactant, and then in 5% O₂ at 400 °C to clean the remaining residue from SWCNTs. This strategy works even for nanotubes of small diameters (~0.78 nm), which are susceptible to thermal oxidation at elevated temperatures. This work provides new insights for the choice or design of surfactants in applications such as electrical sensors, 42,43 printable electronics, and

optoelectronics⁴⁵ where the clean removal of the surfactant after solution processing is key to enhanced device performance.

EXPERIMENTAL SECTION

Synthesis of the ADC Surfactant. Typically, 0.5 g of deoxycholic acid (≥98%, Sigma-Aldrich) and 30 mL of liquid ammonia (mole ratio of 1:9400) were mixed and stirred overnight in a 100 mL round-bottom flask equipped with a condenser filled with dry ice and immersed in a $-40~^{\circ}\text{C}$ ethanol bath. The temperature was then increased to $-30~^{\circ}\text{C}$ to evaporate the excess liquid ammonia (boiling point: $-33.34~^{\circ}\text{C}$). The resulting ADC product was directly collected as a white powder. A 1 wt % aqueous solution of this surfactant was prepared by simply dissolving the powder in water.

Alternatively, we can prepare ADC solution by reacting deoxycholic acid with ammonium hydroxide. For preparing 200 mL of 1 wt % ADC aqueous solution, 2 g of deoxycholic acid was mixed with 98 g of water to form a suspension. We then added 1 mL of ammonium hydroxide (J.T. Baker, ~ 10 to 35% ammonia), which caused deoxycholic acid to completely dissolve (pH = ~ 8 to 9). Then, the concentration of ADC was tuned to 1 wt % by adding 99 g of water.

SWCNT Dispersion. Three sources of SWCNTs, including CoMoCAT SG65 SWCNTs (Southwest Nanotechonologies), EC1.5 (Meijo Nano Carbon Co., Ltd), and EC2.0 (Meijo Nano Carbon Co. Ltd), were used to demonstrate the ability of ADC to disperse SWCNTs. The SWCNT powders were added to 1 wt % ADC aqueous solution at a concentration of 0.7 mg/mL. The mixtures were probe-sonicated for 30 min at 30 W (MiSonix4000 ultrasonicator). The resulting dark solutions were then centrifuged for 1 h at 25 000g (Eppendorf 5417R refrigerated centrifuge) to remove any large undissolved nanotube bundles (Figure 1d). For control groups, SWCNTs were dispersed in 1 wt % DOC (≥98%, Sigma-Aldrich) aqueous solution and in chloroform without surfactants using the same process of tip sonication and centrifugation. Note, in Figure S2, initial solutions were prepared by dissolving 0.5-10 mg of CoMoCAT SG65 SWCNT powder in 1 mL of 1 wt % ADC aqueous solution through tip sonication without centrifugation.

Spectroscopic Characterization. The optical absorption spectra of SWCNT supernatants were measured using a UV-Vis-NIR spectrophotometer (PerkinElmer Lambda 1050) equipped with a broadband InGaAs detector. The PL maps were generated with a NanoLog spectrofluorometer (Horiba Jobin Yvon) using a liquid-N2 cooled InGaAs array. Since the concentrations of initial SWCNT solutions were above the detection limit of the UV-vis-NIR spectrophotometer, the SWCNT solutions were diluted 40- to 400fold to obtain the absorption spectra and PL maps. In Figures 1 and S1, the centrifuged solutions were diluted 40 times for the measurement of absorption and PL maps. FTIR spectra were measured using a Thermo Nicolet NEXUS 670 FTIR with a KBr beam splitter. The scanning range was ~4000 to 650 cm⁻¹. Mass spectra were collected using a JEOL ACCUTOF-CS mass spectrometer with DART ionization sources in positive-ion mode. Raman spectra were measured using a Yvon Jobin LabRam ARAMIS Raman microscope with a 532 nm laser.

Thermogravimetric Analysis and Annealing. To optimize the heat treatment for removing the ADC surfactant and keeping SWCNTs intact, TGA was performed on the ADC powder (synthesized by mixing liquid ammonia and deoxycholic acid) and SWCNTs in Ar (99.999% purity, including 1 ppm of O_2 and 1 ppm of H_2O_3 , Airgas) atmosphere and various oxidizing conditions (oxygen concentration: 1–20%) from 30 to 700 °C at a rate of 5 °C/min. The initial mass of all samples was ~4 to 6 mg, measured in a 70 μ L alumina crucible. TGA was performed on a TGA module (TGA/DSC 2, Mettler Toledo) equipped with a gas controller (GC200).

TEM Observation. A perfect loop was inserted into the SWCNT solution dispersed by ADC, DOC, or chloroform to pick up an ultrathin solution layer that was then transferred on a holy silicon nitride membrane (Ted Pella, Inc., hole size = 200 nm). The silicon nitride membranes with suspended SWCNTs were then annealed in a

tube furnace following the optimized formula (annealing in Ar at 400 $^{\circ}$ C for 1 h and then in 5% O₂ for another 1 h), followed by characterization using a JEOL JEM 2100 LaB6 TEM with 200 kV accelerating voltage.

CNT Electrical Device. Electrodes (10 nm Cr, 60 nm Pt, W = 48 μ m) were fabricated on a Si/SiO₂ wafer by photolithography and ebeam deposition, followed by lift-off processes. The final nanotube channel lengths were ~3 to 10 μ m. We deposited EC1.5 SWCNTs across electrode gaps using electrophoresis at a frequency of 10 MHz and an alternating voltage from -5 to +5 V. The resistance of SWCNT channels were measured using a Keithley 4200 parameter analyzer with a sweep voltage of -1 to +1 V. The morphology of SWCNT channels was characterized by a Hitachi SU-70 FEG SEM with 1.0 kV accelerating voltage.

Hyperspectral Photoluminescence Imaging. A SWCNT film was prepared by filtrating SG65 SWCNT solution dispersed by 1 wt % ADC through an alumina anodisc membrane (Whatman, U.K.). The SWCNT film was then transferred on a sapphire substrate. The hyperspectral imaging was performed on a custom-build microscope. We used an infrared optimized ×50 objective, along with a continuous wave laser at 561 nm (JiveTM Cobolt AB, Sweden) as the excitation light source. PL emission from the sample was filtered through an 870 nm long-pass emission filter.

ASSOCIATED CONTENT

Supporting Information

The Supporting Information is available free of charge at https://pubs.acs.org/doi/10.1021/acs.chemmater.1c00970.

UV-visible absorption spectra, photoluminescence mappings, DART mass spectra, TGA data, TEM images, and Raman spectrum (PDF)

AUTHOR INFORMATION

Corresponding Author

YuHuang Wang — Department of Chemistry and Biochemistry, University of Maryland, College Park, Maryland 20742, United States; Maryland NanoCenter, University of Maryland, College Park, Maryland 20742, United States; orcid.org/0000-0002-5664-1849; Email: yhw@umd.edu

Authors

Chiyu Zhang — Department of Chemistry and Biochemistry, University of Maryland, College Park, Maryland 20742, United States; oorcid.org/0000-0001-6248-7879

Peng Wang – Department of Chemistry and Biochemistry, University of Maryland, College Park, Maryland 20742, United States

Benjamin Barnes – Department of Chemistry and Biochemistry, University of Maryland, College Park, Maryland 20742, United States

Jacob Fortner – Department of Chemistry and Biochemistry, University of Maryland, College Park, Maryland 20742, United States

Complete contact information is available at: https://pubs.acs.org/10.1021/acs.chemmater.1c00970

Notes

The authors declare no competing financial interest.

■ ACKNOWLEDGMENTS

This work is partially supported by the National Science Foundation through grant no. CHE CHE1904488. The authors thank Dr. Yue Li and Dr. Alexandra Brozena for helpful discussions.

REFERENCES

- (1) Dürkop, T.; Getty, S. A.; Cobas, E.; Fuhrer, M. S. Extraordinary Mobility in Semiconducting Carbon Nanotubes. *Nano Lett.* **2004**, *4*, 35–39.
- (2) Bachilo, S. M.; Strano, M. S.; Kittrell, C.; Hauge, R. H.; Smalley, R. E.; Weisman, R. B. Structure-Assigned Optical Spectra of Single-Walled Carbon Nanotubes. *Science* **2002**, *298*, 2361–2366.
- (3) Hu, L.; Hecht, D. S.; Grüner, G. Carbon Nanotube Thin Films: Fabrication, Properties, and Applications. *Chem. Rev.* **2010**, *110*, 5790–5844.
- (4) Fujigaya, T.; Nakashima, N. Non-Covalent Polymer Wrapping of Carbon Nanotubes and the Role of Wrapped Polymers as Functional Dispersants. *Sci. Technol. Adv. Mater.* **2015**, *16*, No. 024802.
- (5) Kang, Y.; Taton, T. A. Micelle-Encapsulated Carbon Nanotubes: A Route to Nanotube Composites. *J. Am. Chem. Soc.* **2003**, *125*, 5650–5651.
- (6) O'Connell, M. J.; Boul, P.; Ericson, L. M.; Huffman, C.; Wang, Y.; Haroz, E.; Kuper, C.; Tour, J.; Ausman, K. D.; Smalley, R. E. Reversible Water-Solubilization of Single-Walled Carbon Nanotubes by Polymer Wrapping. *Chem. Phys. Lett.* **2001**, 342, 265–271.
- (7) Nish, A.; Hwang, J.-Y.; Doig, J.; Nicholas, R. J. Highly Selective Dispersion of Single-Walled Carbon Nanotubes Using Aromatic Polymers. *Nat. Nanotechnol.* **2007**, *2*, 640–646.
- (8) Zheng, M.; Jagota, A.; Semke, E. D.; Diner, B. A.; Mclean, R. S.; Lustig, S. R.; Richardson, R. E.; Tassi, N. G. DNA-Assisted Dispersion and Separation of Carbon Nanotubes. *Nat. Mater.* **2003**, *2*, 338–342.
- (9) O'Connell, M. J.; Bachilo, S. M.; Huffman, C. B.; Moore, V. C.; Strano, M. S.; Haroz, E. H.; Rialon, K. L.; Boul, P. J.; Noon, W. H.; Kittrell, C.; Ma, J.; Hauge, R. H.; Weisman, R. B.; Smalley, R. E. Band Gap Fluorescence from Individual Single-Walled Carbon Nanotubes. *Science* **2002**, 297, 593–596.
- (10) Hersam, M. C. Progress towards Monodisperse Single-Walled Carbon Nanotubes. *Nat. Nanotechnol.* **2008**, *3*, 387–394.
- (11) Wenseleers, W.; Vlasov, I. I.; Goovaerts, E.; Obraztsova, E. D.; Lobach, A. S.; Bouwen, A. Efficient Isolation and Solubilization of Pristine Single-Walled Nanotubes in Bile Salt Micelles. *Adv. Funct. Mater.* **2004**, *14*, 1105–1112.
- (12) Zhang, Q.; Huang, J.-Q.; Qian, W.-Z.; Zhang, Y.-Y.; Wei, F. The Road for Nanomaterials Industry: A Review of Carbon Nanotube Production, Post-Treatment, and Bulk Applications for Composites and Energy Storage. *Small* **2013**, *9*, 1237–1265.
- (13) Lu, W.; Zu, M.; Byun, J.-H.; Kim, B.-S.; Chou, T.-W. State of the Art of Carbon Nanotube Fibers: Opportunities and Challenges. *Adv. Mater.* **2012**, *24*, 1805–1833.
- (14) Wang, P.; Barnes, B.; Huang, Z.; Wang, Z.; Zheng, M.; Wang, Y. Beyond Color: The New Carbon Ink. *Adv. Mater.* **2021**, No. 2005890.
- (15) Choi, S.-J.; Bennett, P.; Takei, K.; Wang, C.; Lo, C. C.; Javey, A.; Bokor, J. Short-Channel Transistors Constructed with Solution-Processed Carbon Nanotubes. *ACS Nano* **2013**, *7*, 798–803.
- (16) Park, J. G.; Smithyman, J.; Lin, C.-Y.; Cooke, A.; Kismarahardja, A. W.; Li, S.; Liang, R.; Brooks, J. S.; Zhang, C.; Wang, B. Effects of Surfactants and Alignment on the Physical Properties of Single-Walled Carbon Nanotube Buckypaper. *J. Appl. Phys.* **2009**, *106*, No. 104310.
- (17) Hu, C.; Yang, C.; Hu, S. Hydrophobic Adsorption of Surfactants on Water-Soluble Carbon Nanotubes: A Simple Approach to Improve Sensitivity and Antifouling Capacity of Carbon Nanotubes-Based Electrochemical Sensors. *Electrochem. Commun.* **2007**, *9*, 128–134.
- (18) Avouris, P.; Freitag, M.; Perebeinos, V. Carbon-Nanotube Photonics and Optoelectronics. *Nat. Photonics* **2008**, *2*, 341–350.
- (19) Fantini, C.; Cassimiro, J.; Peressinotto, V. S. T.; Plentz, F.; Souza Filho, A. G.; Furtado, C. A.; Santos, A. P. Investigation of the Light Emission Efficiency of Single-Wall Carbon Nanotubes Wrapped with Different Surfactants. *Chem. Phys. Lett.* **2009**, 473, 96–101.

- (20) Brege, J. J.; Gallaway, C.; Barron, A. R. Fluorescence Quenching of Single-Walled Carbon Nanotubes in SDBS Surfactant Suspension by Metal Ions: Quenching Efficiency as a Function of Metal and Nanotube Identity. *J. Phys. Chem. C* **2007**, *111*, 17812–17820
- (21) Siitonen, A. J.; Tsyboulski, D. A.; Bachilo, S. M.; Weisman, R. B. Surfactant-Dependent Exciton Mobility in Single-Walled Carbon Nanotubes Studied by Single-Molecule Reactions. *Nano Lett.* **2010**, *10*, 1595–1599.
- (22) Ndiaye, A. L.; Varenne, C.; Bonnet, P.; Petit, E.; Spinelle, L.; Brunet, J.; Pauly, A.; Lauron, B. Elaboration of SWNTs-Based Gas Sensors Using Dispersion Techniques: Evaluating the Role of the Surfactant and Its Influence on the Sensor Response. *Sens. Actuators, B* **2012**, *162*, 95–101.
- (23) Hilmer, A. J.; McNicholas, T. P.; Lin, S.; Zhang, J.; Wang, Q. H.; Mendenhall, J. D.; Song, C.; Heller, D. A.; Barone, P. W.; Blankschtein, D.; Strano, M. S. Role of Adsorbed Surfactant in the Reaction of Aryl Diazonium Salts with Single-Walled Carbon Nanotubes. *Langmuir* **2012**, *28*, 1309–1321.
- (24) Rossi, J. E.; Soule, K. J.; Cleveland, E.; Schmucker, S. W.; Cress, C. D.; Cox, N. D.; Merrill, A.; Landi, B. J. Removal of Sodium Dodecyl Sulfate Surfactant from Aqueous Dispersions of Single-Wall Carbon Nanotubes. *J. Colloid Interface Sci.* **2017**, *495*, 140–148.
- (25) Yun, D.-J.; Kim, J.-M.; Ra, H.; Byun, S.; Kim, H.; Park, G.-S.; Park, S.; Rhee, S.-W. The Physical/Chemical Properties and Electrode Performance Variations of SWNT Films in Consequence of Solution Based Surfactant Elimination Processes. *Org. Electron.* **2013**, *14*, 2962–2972.
- (26) Jo, J. W.; Jung, J. W.; Lee, J. U.; Jo, W. H. Fabrication of Highly Conductive and Transparent Thin Films from Single-Walled Carbon Nanotubes Using a New Non-Ionic Surfactant via Spin Coating. *ACS Nano* **2010**, *4*, 5382–5388.
- (27) Geng, H.-Z.; Kim, K. K.; So, K. P.; Lee, Y. S.; Chang, Y.; Lee, Y. H. Effect of Acid Treatment on Carbon Nanotube-Based Flexible Transparent Conducting Films. *J. Am. Chem. Soc.* **2007**, *129*, 7758–7759
- (28) Zhang, Q.; Vichchulada, P.; Shivareddy, S. B.; Lay, M. D. Reducing Electrical Resistance in Single-Walled Carbon Nanotube Networks: Effect of the Location of Metal Contacts and Low-Temperature Annealing. *J. Mater. Sci.* **2012**, *47*, 3233–3240.
- (29) Brady, G. J.; Way, A. J.; Safron, N. S.; Evensen, H. T.; Gopalan, P.; Arnold, M. S. Quasi-Ballistic Carbon Nanotube Array Transistors with Current Density Exceeding Si and GaAs. *Sci. Adv.* **2016**, *2*, No. e1601240.
- (30) Duque, J. G.; Hamilton, C. E.; Gupta, G.; Crooker, S. A.; Crochet, Jared. J.; Mohite, A.; Htoon, H.; Obrey, K. A. D.; Dattelbaum, A. M.; Doorn, S. K. Fluorescent Single-Walled Carbon Nanotube Aerogels in Surfactant-Free Environments. *ACS Nano* **2011**, *5*, 6686–6694.
- (31) Kane, A. A.; Ford, A. C.; Nissen, A.; Krafcik, K. L.; Léonard, F. Etching of Surfactant from Solution-Processed, Type-Separated Carbon Nanotubes and Impact on Device Behavior. *ACS Nano* **2014**, *8*, 2477–2485.
- (32) Urper, O.; Çakmak, İ.; Karatepe, N. Fabrication of Carbon Nanotube Transparent Conductive Films by Vacuum Filtration Method. *Mater. Lett.* **2018**, 223, 210–214.
- (33) Torrens, O. N.; Milkie, D. E.; Zheng, M.; Kikkawa, J. M. Photoluminescence from Intertube Carrier Migration in Single-Walled Carbon Nanotube Bundles. *Nano Lett.* **2006**, *6*, 2864–2867.
- (34) Jaber-Ansari, L.; Iddir, H.; Curtiss, L. A.; Hersam, M. C. Influence of Electronic Type Purity on the Lithiation of Single-Walled Carbon Nanotubes. *ACS Nano* **2014**, *8*, 2399–2409.
- (35) Tittmann-Otto, J.; Hermann, S.; Kalbacova, J.; Hartmann, M.; Toader, M.; Rodriguez, R. D.; Schulz, S. E.; Zahn, D. R. T.; Gessner, T. Effect of Cleaning Procedures on the Electrical Properties of Carbon Nanotube Transistors—A Statistical Study. *J. Appl. Phys.* **2016**, *119*, No. 124509.

- (36) Dubinsky, S.; Grader, G. S.; Shter, G. E.; Silverstein, M. S. Thermal Degradation of Poly(Acrylic Acid) Containing Copper Nitrate. *Polym. Degrad. Stab.* **2004**, *86*, 171–178.
- (37) McFarlane, S. L.; Piercey, D. G.; Coumont, L. S.; Tucker, R. T.; Fleischauer, M. D.; Brett, M. J.; Veinot, J. G. C. Toward Thermally, Oxidatively, and Spectrally Stable Polyfluorene-Based Materials: Aromatic Ether-Functionalized Polyfluorene. *Macromolecules* **2009**, 42, 591–598.
- (38) Alongi, J.; Di Blasio, A.; Milnes, J.; Malucelli, G.; Bourbigot, S.; Kandola, B.; Camino, G. Thermal Degradation of DNA, an All-in-One Natural Intumescent Flame Retardant. *Polym. Degrad. Stab.* **2015**, 113, 110–118.
- (39) Sreeram, A.; Patel, N. G.; Venkatanarayanan, R. I.; DeLuca, S. J.; Yuya, P. A.; Krishnan, S. Thermogravimetric Study of the Kinetics of Formation of Poly(Para-Phenylene Vinylene) by Thermal Conversion of a Sulfonium Precursor. *Polym. Test.* **2014**, *37*, 170–178
- (40) PubChem. Deoxycholic acid. https://pubchem.ncbi.nlm.nih.gov/compound/222528 (accessed Aug 1, 2020).
- (41) Liew, K. M.; Wong, C. H.; He, X. Q.; Tan, M. J. Thermal Stability of Single and Multi-Walled Carbon Nanotubes. *Phys. Rev. B* **2005**, 71, No. 075424.
- (42) Ng, A. L.; Chen, C.-F.; Kwon, H.; Peng, Z.; Lee, C. S.; Wang, Y. Chemical Gating of a Synthetic Tube-in-a-Tube Semiconductor. *J. Am. Chem. Soc.* **2017**, *139*, 3045–3051.
- (43) Park, S.; Vosguerichian, M.; Bao, Z. A Review of Fabrication and Applications of Carbon Nanotube Film-Based Flexible Electronics. *Nanoscale* **2013**, *5*, 1727–1752.
- (44) Cao, C.; Andrews, J. B.; Franklin, A. D. Completely Printed, Flexible, Stable, and Hysteresis-Free Carbon Nanotube Thin-Film Transistors via Aerosol Jet Printing. *Adv. Electron. Mater.* **2017**, 3, No. 1700057.
- (45) Cao, Q.; Han, S.-J.; Tersoff, J.; Franklin, A. D.; Zhu, Y.; Zhang, Z.; Tulevski, G. S.; Tang, J.; Haensch, W. End-Bonded Contacts for Carbon Nanotube Transistors with Low, Size-Independent Resistance. *Science* **2015**, *350*, 68–72.
- (46) Wu, X.; Kim, M.; Qu, H.; Wang, Y. Single-Defect Spectroscopy in the Shortwave Infrared. *Nat. Commun.* **2019**, *10*, No. 2672.